EFFECTS OF FAN PLACEMENTS ON THERMAL CHARACTERISTICS OF AN AIR-COOLED LITHIUM-ION BATTERY MODULE

Erdi Tosun[1*], Sinan Keyinci[1], Ali Cem Yakaryılmaz[1], Şafak Yıldızhan[1], Mustafa Özcanlı[1], Halil Yüksek[1]

[1]Çukurova University, Faculty of Engineering, Department of Automotive Engineering, 01250, Adana, Turkey

** Corresponding author. Tel.: +90 5068394496*

E-mail addresses: etosun@cu.edu.tr (E. Tosun), skeiyinci@cu.edu.tr (S. Keyinci), acyakaryilmaz@cu.edu.tr (A. C. Yakaryılmaz), ozcanli@cu.edu.tr (M. Özcanlı), yildizhans@cu.edu.tr (Ş. Yıldızhan), halilyuksek190525@gmail.com (H. Yüksek)

Abstract

Effective thermal management is crucial for ensuring the safety, durability, and efficiency of battery systems, particularly under high-load conditions. This research investigates the impact of various fan arrangements on the temperature characteristics of a lithium-ion (LiB) battery module. Three different battery thermal management systems (BTMS) were set and stated as BTMS I, BTMS II, and BTMS III. In BTMS I, one fan was located at the inlet, and a hole was left at the outlet. In BTMS II, two fans were located side by side at the inlet, with the outlet configured the same as in BTMS I. Lastly, in BTMS III, one fan was placed at the inlet, and another at the outlet. Reductions of up to 27.8% in maximum cell temperature (T_{max}) and up to 57.2% in maximum cell-to-cell temperature difference (TD) were achieved with BTMS I and BTMS II, respectively.

Keywords: Battery, BTMS, Cooling, Lithium-ion, Temperature

1. INTRODUCTION

Harmful emissions emitted by internal combustion engines (ICEs), depending on combustion processes, have adverse effects on both the environment and human health in the transportation sector. Recently, the aforementioned notorious effects of ICEs have been the fundamental motivation behind making huge efforts to transition from ICEs to electric vehicles (EVs) in road transport [1]. Not only environmental concerns but also limited fossil fuel reserves have accelerated interest in EVs nowadays [2].

Batteries are at the focal point of EV studies since they supply the energy required for the traction of a vehicle. On the other hand, a considerable amount of EV costs consist of battery prices [3,4]. In recent years, lithium-ion batteries (LiBs) have been preferred instead of lead-acid and nickel-cadmium batteries in EVs. The main reasons LiBs dominate the market are their shorter charging times, longer range, lower prices, and the availability of charging stations compared to lead-acid and nickel-cadmium batteries [5,6].

The temperature sensitivity of LiBs is the most crucial drawback of them. The optimum temperature range for LiB operation is suggested to be 15-35 ºC, with a cell-to-cell variation of less than 5 ºC being desirable [7–9]. The temperature values outside these limits greatly affect battery performance and lifespan. Moreover, security problems may also arise [10–12]. Following Figure 1 summarizes the temperature dependency of LiBs. Above the optimal region, safety issues may arise due to accelerated side reactions, while dropping below the desired range can lead to performance losses due to slower interfacial kinetics and increased electrolyte viscosity [13].

Wang et al. [14] developed a battery module consisting of 30 cylindrical 18650-type cells in a 6-series, 5-parallel configuration, using a forced air-cooling system. Tests at discharge rates of 1C, 1.5C, and 2C showed that without cooling, the maximum temperature (T_{max}) and temperature difference (TD) were 69.8 °C and 17.7 °C, respectively. At a 1C discharge rate (Case 1), T_{max} stayed below 45.0 °C, and TD remained under 5.0 °C, indicating uniform heat dissipation. While high C-rates still caused uneven heat distribution, the forced air-cooling system in Case 1 (upper-opening cross ventilation) proved more effective than in Case 2 (bottom-opening ventilation), demonstrating higher efficiency and a lower TD. Jiaqiang et al. [15] conducted a study to investigate various air-cooling strategies by altering the relative positions of the airflow inlet and outlet to identify the most effective cooling method. The results indicate that positioning the inlet and outlet on opposite sides yields superior cooling performance compared to when they are on the same side. Additionally, the incorporation of a baffle plate significantly enhances the thermal performance of air-cooling strategies with lateral inlet and outlet configurations. Wang et al. [16] investigated air-cooling strategies for various battery module structures by installing fans in different locations to improve temperature uniformity. They concluded that the cooling effectiveness is optimal when the fan is located on the top of the battery module, regardless of the module's structure. Hwang et al. [17] studied the effects of ventilation inlet and outlet locations, as well as gaps between battery cells, on heat dissipation and temperature distribution within a battery pack. Using an existing pack as a baseline, a computational fluid dynamics model analyzed temperature distribution and airflow conditions. The study found that the temperature difference between the highest and lowest

points was reduced by 39%, from 6.04°C to 3.67°C, and the heat dissipation rate improved by 3.8%. Zhang et al. [18] improved air cooling performance by analyzing the effects of the relative position and height of the inlet and outlet, as well as the distribution and spacing of cells. Their study found that, compared to crossed and diagonal configurations on opposite sides, aligning the inlet and outlet on the same side enhances the air-cooling performance of the battery pack. Yang et al. [19] performed a structural optimization study to improve the heat distribution of battery thermal management system (BTMS). Two common BTMSs, specifically the Z-type (BTMS I) and U-type (BTMS II), were selected for investigation. Additionally, two novel structures (BTMS III and BTMS IV) were proposed, including a spoiler at the air inlet manifold of the initial BTMSs to explore the effectiveness of this modification. By studying structural parameters such as spoiler length and height, and spoiler offset distance, optimized versions of BTMS III and BTMS IV called BTMS III-opt and BTMS IV-opt were evaluated. The results showed that after optimization, BTMS III-opt had a T_{max} of 327.43 K and a maximum temperature difference (TD_{max}) of 3.64 K. This means it was 2.56 K cooler and had a 3.44 K smaller TD compared to BTMS I. For BTMS IV-opt, the T_{max} was 326.29 K, and the TD_{max} was 1.19 K, which was 2.79 K cooler and had a 4.98 K smaller TD compared to BTMS II. Wang et al. [20] experimentally studied the reciprocating Z-type air-cooling strategy of BTMS. The parameters such as start time, heating power, period, cooling fan power, and ambient temperature were studied. Additionally, an energy-saving approach using an intermittent strategy was introduced, which could reduce energy consumption by about 10%. Yang et al. [21] investigated forced air-cooled BTMS to manage the temperature uniformity of the battery pack. They theoretically developed a control strategy to provide temperature uniformity through the pack. Three modified BTMS were designed based on conventional Z-type configuration. There were two adjustable valves that were able to regulate airflow. With optimal valve opening value T_{max} and TD_{max} were reduced by 4 K and 5.93 K, respectively.

In this study, various air-cooled BTMSs were applied to a 3S2P battery module. Firstly, the thermal characteristics of the module were revealed under 1C and 2C discharge conditions. three different BTMS were tried by changing fan placements. In BTMS I, one fan was located at the inlet, and a hole was left at the outlet. In BTMS II, two fans were located side by side at the inlet, with the outlet configured the same as in BTMS I. Lastly, in BTMS III, one fan was placed at the inlet, and another at the outlet.

2. MATERIALS AND METHODS

2.1. LiB Module

Figure 2 illustrates the battery cell used in this study and Table 1 shows the specifications of this 18650-type LiB cell.

The battery module was designed in a 3S2P configuration as shown in Figure 3. The nominal capacity was increased to 5600 mAh with this type of connection.

Cells were spot-welded with nickel strips in the specified configuration after being placed in a 3D-printed battery holder. The perspective and top views of the assembled module are shown in Figure 4, with each cell numbered.

2.2. Experimental Procedure

Five different experiments were performed. In this study, each test was conducted three times under the same operating conditions, and average values were used to ensure the reliability and accuracy of the results. Firstly, the temperature reaction of the battery module to 1C and 2C discharge conditions was revealed as shown in Figure 5.

The charging and discharging processes were performed by the devices with the technical specifications given below in Table 2 and Table 3, respectively. They are demonstrated in Figure 6. At the beginning of each experiment, the module was charged up to 12.6 V and discharged down to 7.5 V. Thermal reaction of the module was observed between 12.6 V (fully charged) and 7.5 V (fully discharged) voltage levels.

During the discharge period, the temperature of each cell in a battery module was monitored using thermocouples, and data were recorded at 10-second intervals with the utilization of a datalogger and thermocouples shown in Figure 7. Technical details of the datalogger and thermocouples were supplied in the following Table 4 and Table 5.

It was observed that there was excessive temperature rise in 2C condition. The cell temperatures increased approximately from 25 ºC to 48 ºC levels. This situation has made the implementation of a BTMS for the battery module under these conditions inevitable. Figure 8 shows the experiments conducted in this study. Besides that, Figure 9 presents BTMS I, BTMS II, and BTMS III during their operation.

Three different BTMSs given in the following Figure 10 were created by plexiglass with different fan locations to perform experiments. In each BTMS, fans were symmetrically located in the middle of both the inlet and outlet. The width (W), height (H), and length (L) of the cabin are 320 mm, 200 mm, and 500 mm, respectively. The thickness of each plate of the cabin is 3 mm. The inlets of BTMS I and BTMS II were designed to host one and two fans. A circular area (160 mm diameter) was left at the outlet. BTMS III was configured with one fan at the

inlet, and another at the outlet. Figure 11 and Table 6 demonstrate the fan and technical details of it, correspondingly.

2.3. Uncertainty Analysis

Conducting uncertainty analysis for the experimental procedure is crucial to enhance the reliability of the results. Errors, which are inherent in any experimental setup, primarily stem from the limitations of the instruments utilized. The uncertainty values of each measurement parameter in the system have been determined with respect to their accuracy values. Percentage uncertainties of battery thermocouple (T_{btc}), ambient thermocouple (T_{atc}), datalogger (DL), and electronic load (EL) were calculated as 1%, 2%, 0.8%, and 1.7%, respectively. Based on these values, the overall uncertainty of the experimental system was derived to be 2.92% using Equation 1:

$$Percent\ of\ \ overall\ uncertainty = \sqrt{\left(T_{btc}\right)^2 + \left(T_{atc}\right)^2 + \left(DL\right)^2 + \left(EL\right)^2} \quad (1)$$

3. RESULTS AND DISCUSSIONS

All tests were conducted at approximately 25 °C ambient temperature. The temperature variations with no BTMS system for 1C and 2C discharge rates were given in Figure 12 and Figure 13. The figures also showed how the TD from cell-to-cell changes every 10 seconds. The cell-to-cell TD represents the variation between the highest and lowest cell temperatures measured at any given time, specifically the difference between the maximum and minimum temperatures among the six cells at a particular moment. This metric is critical as it highlights the uniformity of thermal behavior within the module, which directly impacts performance, safety, and lifespan. The majority of the literature indicates that for optimal operation, batteries should remain between 15-35 °C, and the TD from cell-to-cell should not exceed 5 °C [22–24]. As seen in Figure 12, the T_{max} values were between 31.43 - 34.21 °C for different cells at the end of the discharging period for 1C discharge rate. Although the T_{max} values for each cell occur at the end of the discharging period, TD_{max} between cell-to-cell was observed earlier as 3.12 °C. These temperature levels meet the desired values and fall into the optimum range. On the other hand, when the discharge current was doubled (2C load conditions), the requirement for BTMS became inevitable since the temperature criteria could not be met for T_{max}. Figure 13 illustrates temperature and TD variations during 2C discharge. T_{max} values varied between 43.89 °C - 48.54 °C whereas TD_{max} was 4.65 °C. Under 2C condition, TD_{max} was observed at the end of discharge, unlike at 1C.

Three different BTMSs were designed and tested in order to remove excessive heat generated under 2C discharge condition. In BTMS I, one fan was used at the inlet to blow air onto the battery module, and a circular hole was left at the outlet to expel the heat-extracted air. In BTMS I, T_{max} values were kept between 29.53 - 35.04 °C for different cells while TD_{max} was 5.51 °C at the end of the discharging period as seen in Figure 14. According to the experimental results, values nearly fell within the appropriate range, while TD_{max} value did not. The cooling effect on the battery module under 2C conditions was clearly noticeable as seen from the T_{max} values in the operation of BTMS I. The T_{max} was reduced from 48.54°C to 35.04°C, representing a reduction of 27.8%. Besides that, the possible cause of the deterioration in TD_{max} (18.5% increment) could be that the fan is positioned in the center, resulting in non-uniform cooling of the batteries, especially from the sides of the module.

A noticeable improvement in TD_{max} value stands out in above Figure 15. A wider cooling area, including the front and both sides of the battery, can be provided with the use of two fans side by side. T_{max} values were between 35.18 - 37.16 °C for different cells at the end of the discharging period. Although the T_{max} values for each cell occur at the end of the discharge, the TD_{max} between cell-to-cell was observed earlier as 1.99 °C. TD_{max} obtained under BTMS II was the best result of all. In comparison to 2C with no cooling condition, T_{max} was reduced from 48.54°C to 37.16 °C which corresponds to a 23.44% decrement. The decrease in TD_{max} value, which resulted in the most uniform temperature distribution between cells, was 57.2% compared to 2C test condition with no cooling.

Figure 16 illustrates the temperature results of BTMS III. T_{max} values at the end of discharge varied between 34.87 - 38.75 °C for various cells. A 20.17% reduction in T_{max} (from 48.54 to 38.75 °C) was obtained with this BTMS design. TD_{max} between cell-to-cell was seen earlier than the end of discharge as 4.02 °C and the enhancement for TD_{max} was 13.55%.

1C discharge tests were not conducted under BTMS configurations because cell temperatures stayed below 35°C, which is within the safe operating range, while 2C discharge tests required BTMS implementation due to higher temperature increases. Figure 17 revealed the cell-based T_{max} values in each condition. Although all three BTMSs have achieved a significant reduction in temperature levels under the 2C condition, BTMS I has ensured that the temperature values remain within the optimal range indicated by the green zone. The T_{max} and TD_{max} values obtained in all tests were summarized and presented in Table 7. The TD criterion was satisfied for BTMS II and BTMS III; however, it was not achieved for BTMS I.

4. CONCLUSIONS

This study exhibits the critical role of BTMS in maintaining optimal battery performance, particularly under high discharge conditions. The results indicate that while the battery module remained within acceptable temperature ranges at a 1C discharge rate without additional cooling, the 2C discharge rate necessitated a BTMS due to the significant rise in temperature. Among the three BTMS designs tested, BTMS II provided the most effective cooling, achieving the lowest TD_{max} between cells and the most uniform temperature distribution. Although all BTMS designs successfully reduced the T_{max}, only BTMS II and BTMS III met the TD criterion. These findings highlight the importance of uniform cooling in BTMS design to ensure both optimal temperature levels and uniformity across the battery cells.

The battery module maintained a T_{max} of 34.21 °C and a TD_{max} of 3.12 °C under 1C discharge conditions without any cooling, indicating acceptable performance even without additional thermal management. However, at a 2C discharge rate, T_{max} significantly increased to 48.54 °C, and TD_{max} reached 4.65 °C, highlighting the necessity of BTMS integration under higher thermal loads. Among the tested BTMS configurations, BTMS I reduced T_{max} to 35.04 °C but resulted in a higher TD_{max} of 5.51 °C. BTMS II, despite a slightly higher T_{max} of 37.16 °C, achieved the most uniform temperature distribution with a TD_{max} of 1.99 °C. Meanwhile, BTMS III offered performance with a T_{max} of 38.75 °C and a TD_{max} of 4.02 °C. These comparisons validate the critical role of BTMS in managing thermal loads effectively and underscore the superiority of BTMS II in achieving temperature uniformity across cells.

Nomenclature

BTMS	Battery thermal management system
EV	Electric vehicle
ICE	Internal combustion engines
LiB	Lithium-ion battery
T_{max}	Maximum temperature
TD	Temperature difference
TD_{max}	Maximum temperature difference

ACKNOWLEDGMENTS

This research was supported by Çukurova University Scientific Research Project Unit with FBA-2022-15234 project code.

REFERENCES

1. Farjam, T., Foumani, M. S., and Delkhosh, M. “Optimization of multiple transmission layouts for minimal energy consumption of a battery electric vehicle”, *Sci. Iran.*, **26**(4),

pp. 2382–2393 (2019). DOI: https://doi.org/10.24200/sci.2018.20783

2. Ullah, S., Hayat, R., Zeb, K., et al. "Super-twisting sliding mode controller for energy storage system of a novel multisource hybrid electric vehicle: Simulation and hardware validation", *Int. J. Hydrogen Energy*, **71**, pp. 952–963 (2024). DOI: https://doi.org/10.1016/j.ijhydene.2024.05.326
3. Pla, B., Bares, P., Aronis, A. N., et al. "Leveraging battery electric vehicle energy storage potential for home energy saving by model predictive control with backward induction", *Appl. Energy*, **372**, pp. 123800 (2024). DOI: https://doi.org/10.1016/j.apenergy.2024.123800
4. Yang, C. "Running battery electric vehicles with extended range: Coupling cost and energy analysis", *Appl. Energy*, **306**, pp. 118116 (2022). DOI: https://doi.org/10.1016/j.apenergy.2021.118116
5. Kök, C. and Alkaya, A. "Investigation of Thermal Behavior of Lithium-Ion Batteries under Different Loads", *Eur. Mech. Sci.*, **4**(3), pp. 96–102 (2020). DOI: https://doi.org/10.26701/ems.635707
6. Dehghani, F., Eslamloueyan, R., and Sarshar, M. "A hybrid model for simulation of lithium-ion batteries using artificial neural networks and computational fluid dynamics", *Sci. Iran.*, **29**(6), pp. 3208–3217 (2022). DOI: https://doi.org/10.24200/SCI.2022.59292.6160
7. Bibin, C., Vijayaram, M., Suriya, V., et al. "A review on thermal issues in Li-ion battery and recent advancements in battery thermal management system", *Mater. Today Proc.*, **33**, pp. 116–128 (2020). DOI: https://doi.org/10.1016/j.matpr.2020.03.317
8. Kumar, R. and Goel, V. "A study on thermal management system of lithium-ion batteries for electrical vehicles: A critical review", *J. Energy Storage*, **71**, pp. 108025 (2023). DOI: https://doi.org/10.1016/j.est.2023.108025
9. Singh, L. K., Kumar, R., Gupta, A. K., et al. "Computational study on hybrid air-PCM cooling inside lithium-ion battery packs with varying number of cells", *J. Energy Storage*, **67**, pp. 107649 (2023). DOI: https://doi.org/10.1016/j.est.2023.107649
10. Yazıcı, M. Y. "Thermal Management of Small-Scale Li-ion Battery Module Using Graphite Matrix Composite with Phase Change: Effect of Discharge Rate", *Iğdır Üniversitesi Fen Bilim. Enstitüsü Derg.*, **12**(1), pp. 389–402 (2022). DOI: https://doi.org/10.21597/jist.952021
11. Airò Farulla, G., Palomba, V., Alosio, D., et al. "Optimal design of lithium ion battery

thermal management systems based on phase change material at high current and high environmental temperature", *Therm. Sci. Eng. Prog.*, **42**, pp. 101862 (2023). DOI: https://doi.org/10.1016/j.tsep.2023.101862

12. Jiang, Z. Y., Li, H. B., Qu, Z. G., et al. "Recent progress in lithium-ion battery thermal management for a wide range of temperature and abuse conditions", *Int. J. Hydrogen Energy*, **47**(15), pp. 9428–9459 (2022). DOI: https://doi.org/10.1016/j.ijhydene.2022.01.008
13. Wang, J., Huang, W., Pei, A., et al. "Improving cyclability of Li metal batteries at elevated temperatures and its origin revealed by cryo-electron microscopy", *Nat. Energy*, **4**, pp. 664–670 (2019). DOI: https://doi.org/10.1038/s41560-019-0413-3
14. Wang, Y. W., Jiang, J. M., Chung, Y. H., et al. "Forced-air cooling system for large-scale lithium-ion battery modules during charge and discharge processes", *J. Therm. Anal. Calorim.*, **135**, pp. 2891–2901 (2019). DOI: https://doi.org/10.1007/s10973-018-7646-4
15. Jiaqiang, E., Yue, M., Chen, J., et al. "Effects of the different air cooling strategies on cooling performance of a lithium-ion battery module with baffle", *Appl. Therm. Eng.*, **144**, pp. 231–241 (2018). DOI: https://doi.org/10.1016/j.applthermaleng.2018.08.064
16. Wang, T., Tseng, K. J., Zhao, J., et al. "Thermal investigation of lithium-ion battery module with different cell arrangement structures and forced air-cooling strategies", *Appl. Energy*, **134**, pp. 229–238 (2014). DOI: https://doi.org/10.1016/j.apenergy.2014.08.013
17. Hwang, H.-Y., Chen, Y.-S., and Chen, J.-S. "Optimizing the Heat Dissipation of an Electric Vehicle Battery Pack", *Adv. Mech. Eng.*, **7**(1), pp. 204131 (2015). DOI: https://doi.org/10.1155/2014/204131
18. Zhang, L., Chen, Q., and Wang, T. "Effects of air cooling structure on cooling performance enhancement of prismatic lithium-ion battery packs based on coupled electrochemical-thermal model", *Energy Sci. Eng.*, **9**(9), pp. 1450–1464 (2021). DOI: https://doi.org/10.1002/ese3.905
19. Yang, C., Xi, H., and Wang, M. "Structure optimization of air cooling battery thermal management system based on lithium-ion battery", *J. Energy Storage*, **59**, pp. 106538 (2023). DOI: https://doi.org/10.1016/j.est.2022.106538
20. Wang, C., Xu, J., Wang, M., et al. "Experimental investigation on reciprocating air-cooling strategy of battery thermal management system", *J. Energy Storage*, **58**, pp. 106406 (2023). DOI: https://doi.org/10.1016/j.est.2022.106406

21. Yang, R., Wang, M., and Xi, H. “Thermal investigation and forced air-cooling strategy of battery thermal management system considering temperature non-uniformity of battery pack”, *Appl. Therm. Eng.*, **219**, pp. 119566 (2023). DOI: https://doi.org/10.1016/j.applthermaleng.2022.119566

22. Al-Zareer, M., Dincer, I., and Rosen, M. A. “Comparative assessment of new liquid-to-vapor type battery cooling systems”, *Energy*, **188**, pp. 116010 (2019). DOI: https://doi.org/10.1016/j.energy.2019.116010

23. Liang, L., Zhao, Y., Diao, Y., et al. “Inclined U-shaped flat microheat pipe array configuration for cooling and heating lithium-ion battery modules in electric vehicles”, *Energy*, **235**, pp. 121433 (2021). DOI: https://doi.org/10.1016/j.energy.2021.121433

24. Chen, D., Jiang, J., Kim, G. H., et al. “Comparison of different cooling methods for lithium ion battery cells”, *Appl. Therm. Eng.*, **94**, pp. 846–854 (2016). DOI: https://doi.org/10.1016/j.applthermaleng.2015.10.015

FIGURE CAPTIONS

TABLE CAPTIONS

FIGURES

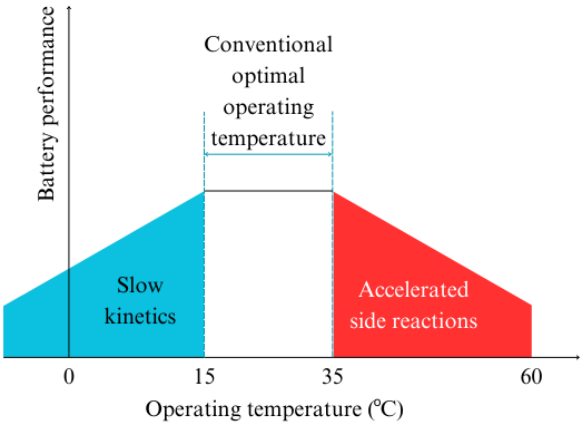

Figure 1. Optimum battery operating temperature ranges [13]

Figure 2. Aspilsan INR18650A28

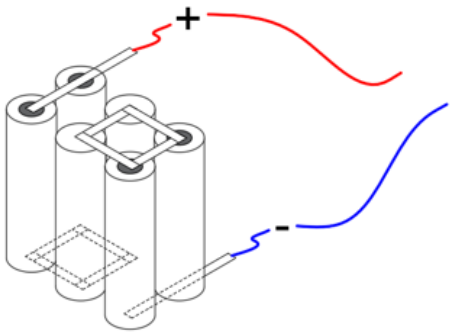

Figure 3. 3S2P battery module configuration

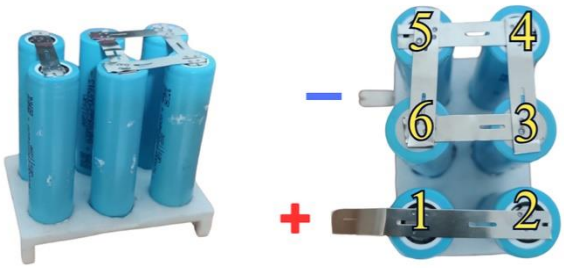

Figure 4. Perspective and top views of the module

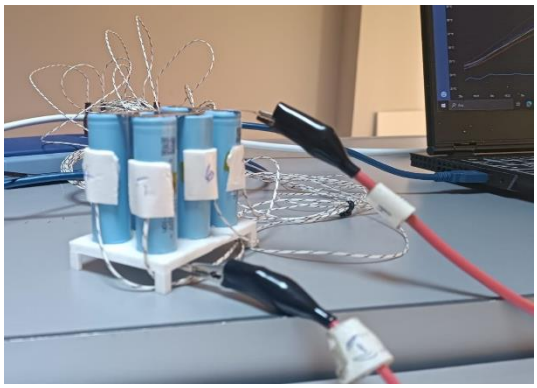

Figure 5. Experiment with no BTMS system

(i)

(ii)

Figure 6. (i) DC Power supply (ii) electronic load

Figure 7. Temperature datalogger with connected thermocouples

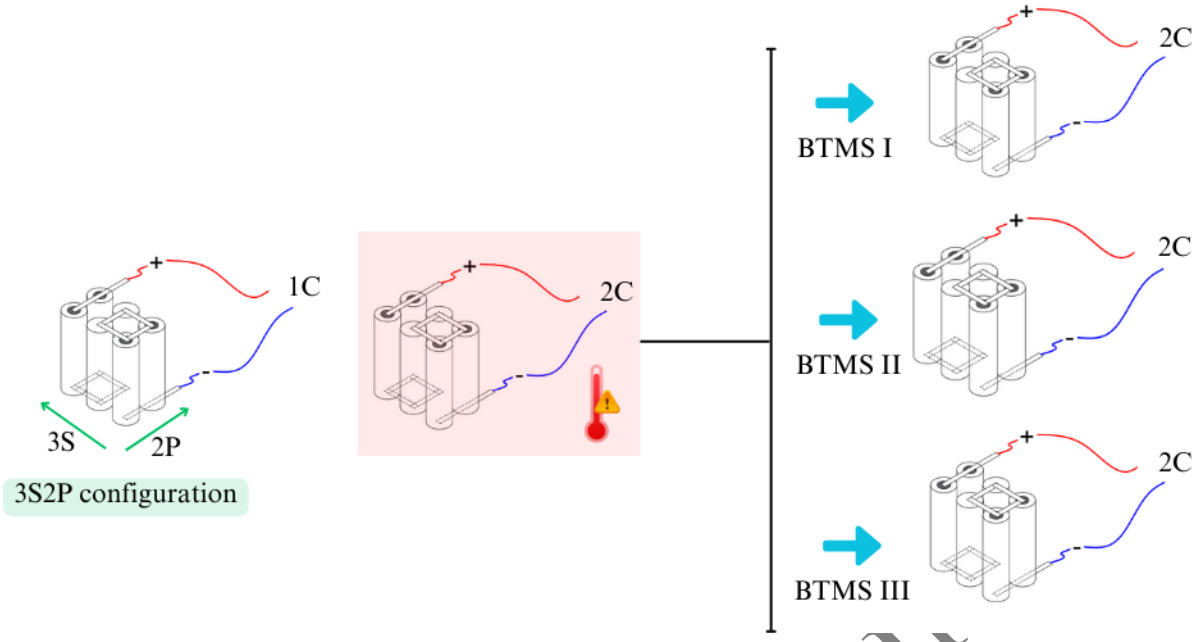

Figure 8. Experiment history

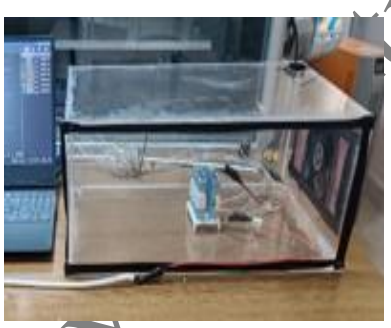

(i)

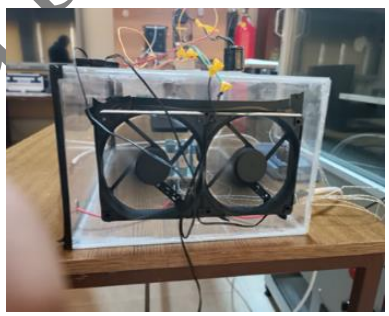

(ii)

(iii)

Figure 9. Tests conducted with (i) BTMS I (ii) BTMS II (iii) BTMS III

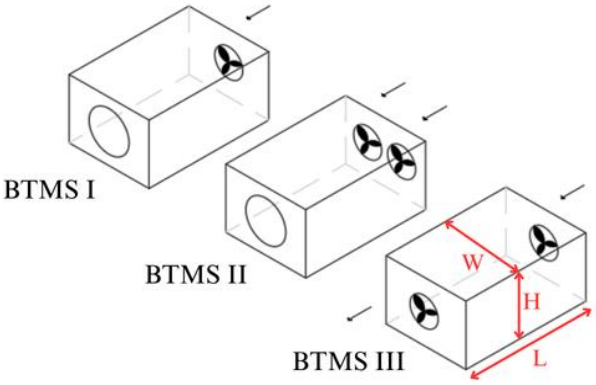

Figure 10. BTMSs with different fan placements

Figure 11. The fan used in experiments

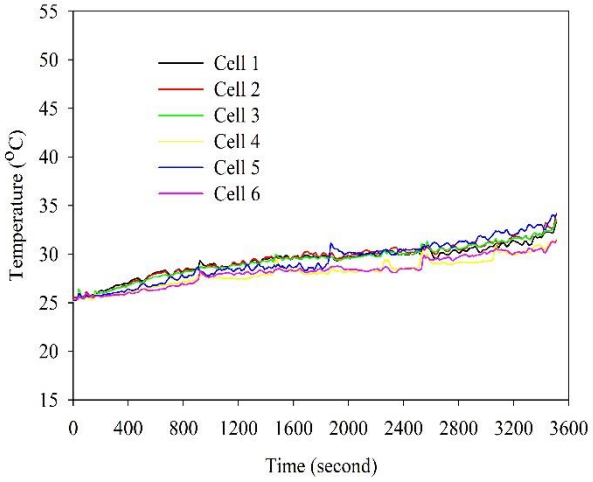

(i)

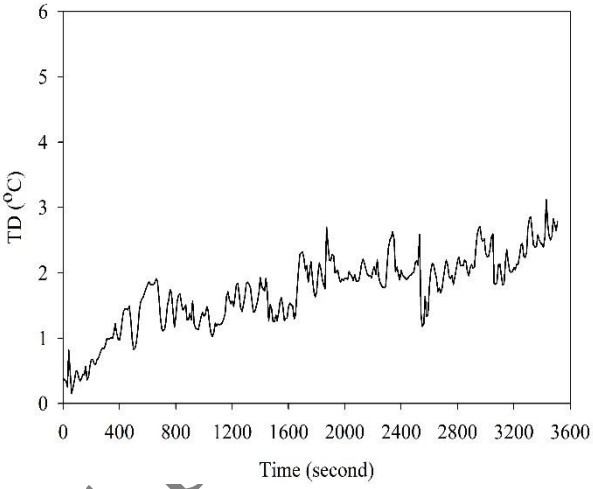

(ii)

Figure 12. 1C discharge with no BTMS (i) cell temperatures (ii) cell-to-cell TD

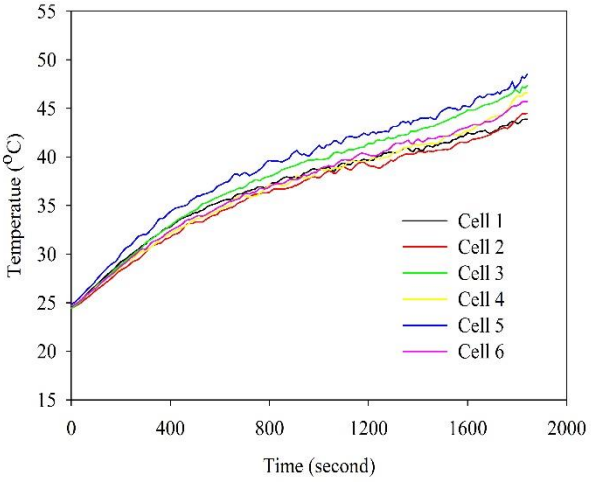

(i)

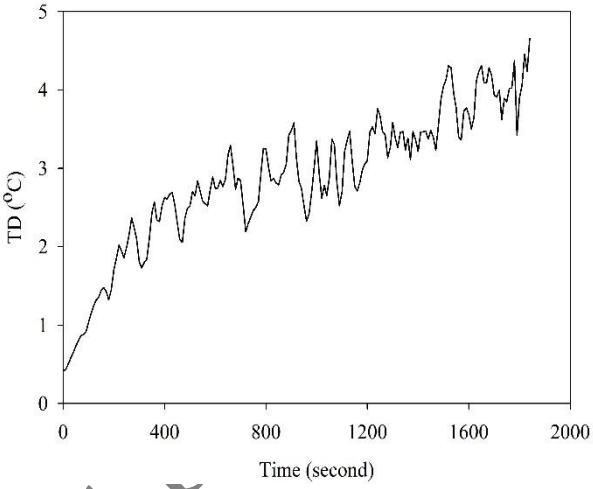

(ii)

Figure 13. 2C discharge with no BTMS (i) cell temperatures (ii) cell-to-cell TD

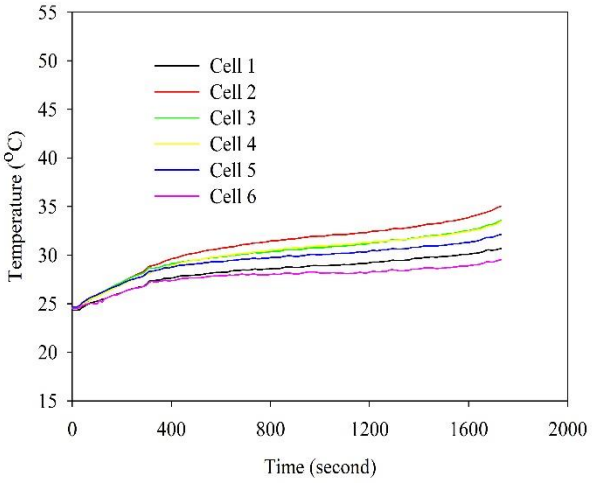

(i)

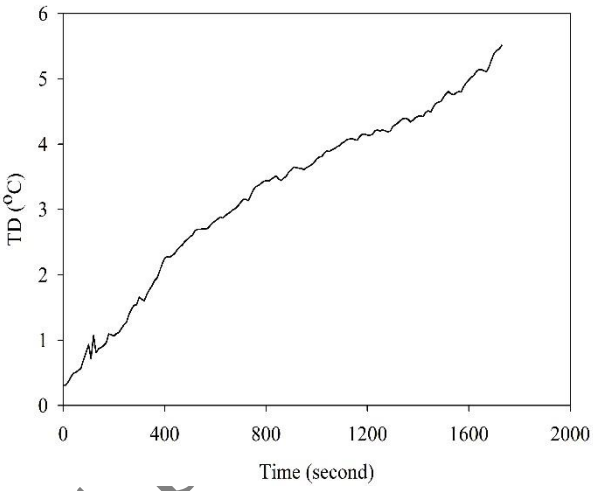

(ii)

Figure 14. 2C discharge with BTMS I (i) cell temperatures (ii) cell-to-cell TD

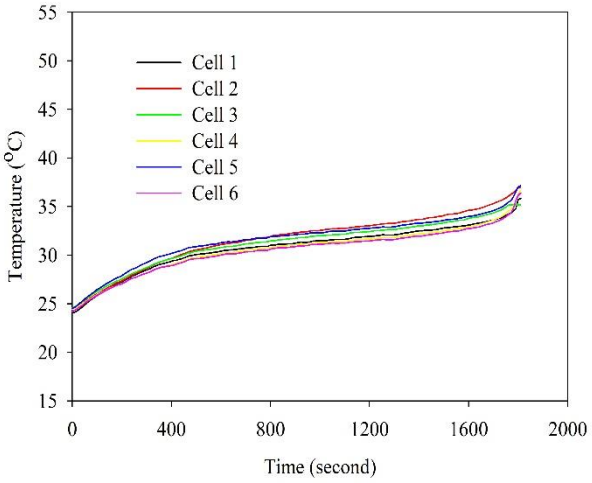

(i)

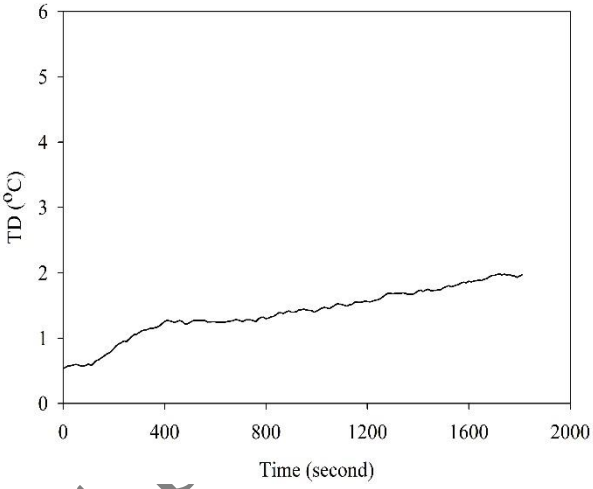

(ii)

Figure 15. 2C discharge with BTMS II (i) cell temperatures (ii) cell-to-cell TD

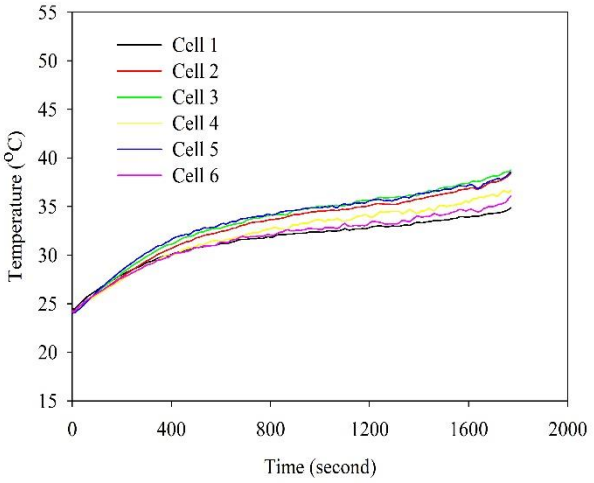

(i)

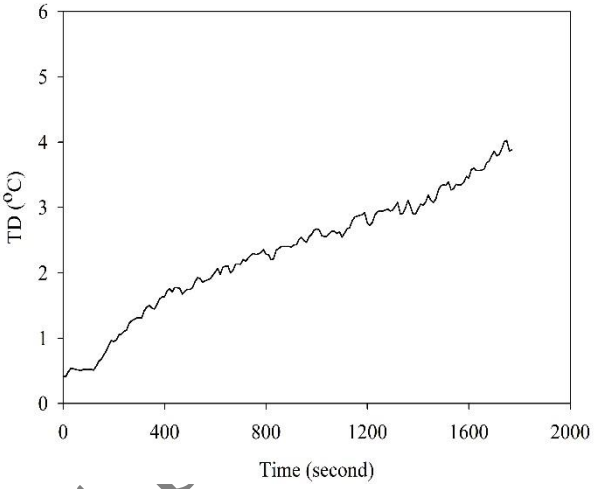

(ii)

Figure 16. 2C discharge with BTMS III (i) cell temperatures (ii) cell-to-cell TD

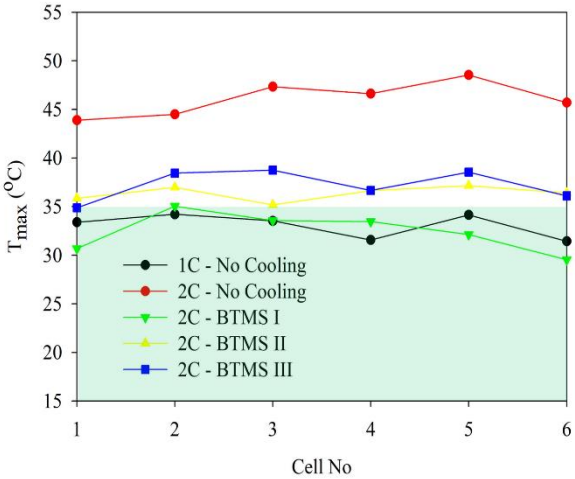

Figure 17. T_{max} values of each cell under various discharge conditions and fan configurations

TABLES

Table 1. Specifications of LiB cell

Brand/Model	:	Aspilsan/INR18650A28
Capacity	:	2800 mAh (Nominal) - 2700 mAh (Minimum)
Nominal voltage	:	3.65 V
End voltage	:	4.2 V (Charge) - 2.5 V (Discharge)
Energy density	:	230 Wh/kg (Gravimetric) - 605 Wh/L (Volumetric)
Weight	:	44.5 ± 0.7 g
Dimensions	:	18.3 + 0.1/-0.2 mm (Diameter) 65 ± 0.2 mm (Height)

Table 2. Technical data of programmable DC power supply

Brand	:	GW Instek PSU 100-15
Rated output voltage	:	100 V
Rated output current	:	15 A
Rated output power	:	1500 W
Load regulation	:	Voltage: 12 mV, Current: 8 mA
Line regulation	:	Voltage: 12 mV, Current: 3.5 mA
Transient response time	:	1 ms
Operating temperature	:	0 to 50 °C

Table 3. Technical data of electronic load

Brand	:	Heliocentris EL 1500
Input voltage	:	230 V / 115 V
Operating temperature	:	0 - 35 ºC
Load voltage	:	1 - 75 V_{DC}
Load current	:	1 - 100 A_{DC}
Load resistance	:	0.02 - 10 kΩ
Power max.	:	1500 W
Dimensions	:	250 x 220 x 440 mm
Weight	:	12 kg

Table 4. Technical data of thermocouple datalogger

Brand	:	Pico TC-08
Number of channels	:	8
Temperature accuracy	:	The sum of ±0.2% of reading and ±0.5 °C
Voltage accuracy	:	The sum of ±0.2% of reading and ±10 µV
Overload protection	:	±30 V
Input range (voltage)	:	±70 mV
Reading rate	:	Up to 10 per second
Operation temperature	:	0 °C to 50 °C
Dimensions	:	201 x 104 x 34 mm

Table 5. Technical data of thermocouple

Brand	:	Pico
Type	:	T
Temperature range	:	-75 °C to 260 °C
Accuracy	:	-40 °C to 125 °C: ±0.5 °C 125 °C to 260 °C: ±0.4 %

Tip construction	:	Exposed junction/welded tip
Cable material	:	Fiberglass
Length	:	3 m

Table 6. Technical details of the fan

Brand/Model	:	Zauss/Z-101
Rated voltage	:	DC 12 V
Rated current	:	0.3 A
Fan speed	:	1600 rpm
Airflow	:	74 CFM
Dimensions	:	120 x 120 x 25 mm

Table 7. T_{max} and TD_{max} values obtained during experiments

Discharge Rate	Cooling	T_{max} (ºC)	TD_{max} (ºC)
1C	No	34.21	3.12
2C	No	48.54	4.65
2C	BTMS I	35.04	5.51
2C	BTMS II	37.16	1.99
2C	BTMS III	38.75	4.02

BIOGRAPHIES

Erdi Tosun is an Assistant Professor of the Department of Automotive Engineering, Çukurova University, Adana, Türkiye. He received his PhD in Mechanical Engineering from Çukurova University in 2018. His research interests include alternative fuels, internal combustion engines, electric vehicles, and lithium-ion batteries.

Sinan Keyinci is an Assistant Professor of the Department of Automotive Engineering, Çukurova University, Adana, Türkiye. He received his PhD in Automotive Engineering from Çukurova University in 2021. His research interests include fuel cells, hybrid propulsion systems, electric vehicles, and lithium-ion batteries.

Ali Cem Yakaryılmaz is a Research Assistant of the Department of Automotive Engineering, Çukurova University, Adana, Türkiye. He received his PhD in Automotive Engineering from Çukurova University in 2025. His research interests include fuel cell, internal combustion engines, electric vehicles, and lithium-ion batteries.

Şafak Yıldızhan enrolled to MSc education in the Automotive Engineering Department of Çukurova University in 2014 and graduated in 2017. Then, he received his PhD in Automotive Engineering from Çukurova University in 2020. His research topics stand out as internal combustion engines, composite materials, and lithium-ion batteries.

Mustafa Ozcanli was born in Adana on May 2, 1977. He completed his PhD in Mechanical Engineering at Çukurova University in 2009. He is also the Head of the Department of Automotive Engineering at Çukurova University, where he serves as Professor Doctor. His research topics stand out as internal combustion engines, biofuels, and composite materials.

Halil Yüksek started his BSc education in 2020 at Çukurova University, Automotive Engineering Department, and is still continuing his BSc education. His research interests include lithium-ion batteries.